Construction and Building Materials 196 (2019) 362–374

Contents lists available at ScienceDirect

Construction and Building Materials

journal homepage: www.elsevier.com/locate/conbuildmat

Analysis of the temperature effect on concrete crosstie flexural behavior

Alvaro E. Canga Ruiz [a], Yu Qian [b,*], J. Riley Edwards [c], Marcus S. Dersch [c]

[a] Arup, 77 Water St, New York, NY 10005, United States
[b] Department of Civil and Environmental Engineering, University of South Carolina, 300 Main Street, Columbia, SC 29208, United States
[c] Rail Transportation and Engineering Center – RailTEC, Department of Civil and Environmental Engineering, University of Illinois at Urbana-Champaign, 205 N. Mathews Ave., Urbana, IL 61801, United States

HIGHLIGHTS

- Temperature at top and base of concrete crossties are linearly related to ambient.
- Change in support conditions due to temperature gradient affects flexural behavior of crossties.
- Relation between temperature gradient and bending moment variation under train loading is linear.
- Curling due to temperature gradient can increase flexural demand up to 38 kip-in at center and rail seats.
- Temperature gradient can lead to a reduction of the flexural capacity of concrete crossties as high as 21%.

ARTICLE INFO

Article history:
Received 13 June 2018
Received in revised form 18 October 2018
Accepted 7 November 2018
Available online 22 November 2018

Keywords:
Concrete
Temperature gradient
Railroad crossties
Railroad sleepers
Bending moments

ABSTRACT

The manner in which temperature affects concrete components or structures has been studied extensively for many applications, such as pavements, bridges, and frames. However, little attention has been given to the temperature effects on concrete railroad crossties. Recent research at the University of Illinois at Urbana-Champaign revealed the relationship between temperature gradient and curling on freight railroad concrete crossties, which showed that temperature gradient could change the support conditions of the crossties, affecting their flexural performance. This paper presents the results from an extensive field study of temperature effects on the flexural behavior of rail transit concrete crossties, part of a larger research program aimed at designing more efficient and resilient concrete crossties for rail transit applications. Field instrumentation was installed on light, heavy, and commuter rail systems to monitor temperature variation and corresponding concrete crosstie flexural behavior for up to 10 months at each location. A linear relationship between the temperature in the crosstie and the ambient temperature is observed. Additionally, the bending moment distribution under revenue service loading conditions is found to be directly affected by the temperature gradient between top and bottom of the crosstie. This effect is believed to be a consequence of the variation in the support condition due to curling, and is thought to be independent of the crosstie design or loading environment. A linear correlation between the temperature gradient variation in the crosstie and the flexural behavior of the crosstie is observed. A maximum difference of 38 kip-in (4.29 kN-m) for the center negative bending moment of the concrete crosstie was found due to a change in the temperature gradient from −10 °F (−5.6 °C) to 37 °F (20.6 °C), which represents 21% of the design capacity. Based on the analysis of field observations, a correction factor of 1 kip-in/°F (0.203 kN-m/°C) is recommended to account for the temperature gradient as a design variable for future rail transit concrete crossties.

1. Introduction

Ballasted track is the most extensive type of railroad track structure both in North America and throughout the world. As one of the key components in the ballasted track, crossties (also known as sleepers) are installed perpendicular to the track. They are embedded in the ballast and the rail is connected to them with fasteners. Crossties are expected to transfer and distribute wheel loads from the rail to the ballast, restrain the track against lateral, longitudinal, and vertical movement, and maintain track gauge [1]. Crossties are primarily subjected to bending due to their loading and support conditions, similar to beam elements. Even though

* Corresponding author.
E-mail addresses: cangaru2@illinois.edu (A.E. Canga Ruiz), yuqian@sc.edu (Y. Qian), jedward2@illinois.edu (J.R. Edwards), mdersch2@illinois.edu (M.S. Dersch).

https://doi.org/10.1016/j.conbuildmat.2018.11.065
0950-0618/

concrete crossties represent a small portion of the market when compared with timber crossties, the number of concrete crossties is increasing and concrete crossties are typically installed in demanding track locations having high curvature and high axle loads [2].

Temperature imposed strains and stresses have been shown to have a significant influence on concrete structures. Studies on prestressed concrete girders [3], concrete frames [4,5], concrete slabs [6–11], and concrete crossties [12] have been conducted in the past, addressing the specific problems and challenges that each component incurs. Issues such as excessive stresses due to the indeterminacy of the structure [3,4,9], excessive deformation or deflection [3,7,13], or the effect in the variation of support conditions [10] are found on different concrete components. Unfortunately, the design of concrete crossties still relies heavily on both experience and empirical results [14]. The current design standards or recommendations are load-based approaches, such as the American Railway Engineering and Maintenance-of-Way Association (AREMA) Manual for Railway Engineering (MRE), EuroNorm (EN) 13230, International Union of Railways (UIC) 713R, and Australian Standard (AS) 1085.14. The support conditions for crossties are oversimplified in those standards or recommendations. Moreover, the influence of temperature on concrete crosstie flexural performance has not been investigated thoroughly, which could lead to unexpected, premature failure. Different from the design approaches for concrete crossties, design standards used for other concrete components or structures in North America do consider the effects of support conditions and temperature variation. For example, the American Association of State Highway and Transportation Officials (AASHTO) includes a chapter in the highway bridge design specifications that addresses the loads induced by temperature effects [15]. Additionally, previous research conducted on the effect of temperature on concrete crossties did prove that the temperature gradient would affect the crosstie bending stress distribution [12]. However, a solution to compensate for the temperature effect was not proposed.

This paper presents the results from an extensive field study of temperature effects on the flexural behavior of rail transit concrete crossties. It is part of a large research program funded by the Federal Transit Administration (FTA), aimed at designing more efficient and resilient concrete crossties for rail transit applications. Specifically, the temperature distribution in concrete crossties exposed to different environmental conditions and the effect of temperature on concrete crosstie flexural performance under rail transit revenue service train operation was investigated. Based on the analysis from field observations, a correction factor is recommended to account for the temperature gradient as a design variable for future rail transit concrete crossties.

2. Field experimentation

In this study, field instrumentation was deployed on tracks owned and operated by three different rail transit agencies during normal revenue service operations (Fig. 1).

Track sections in a light rail system (St. Louis MetroLink), a heavy rail system (MTA New York City Transit Authority), and a commuter rail system (Chicago Metra) operating on infrastructure owned by a Class I freight railroad, were selected. The light rail site at St. Louis MetroLink (hereafter referred as MetroLink) is located in East St. Louis, IL. It is located in a tangent with a speed limit of 55 mph (89 km/h). The heavy rail site (NYCTA) is a curve site at Far Rockaway, NY, where the track speed is limited to 30 mph (48 km/h). The commuter rail site, which is part of the Chicago Metra system (hereafter referred as Metra), is a shared corridor where both freight and commuter rail trains operate. The test site is near Elburn, IL, and it is a tangent track where the track speed is 70 mph (113 km/h).

Each system uses different types of concrete crossties based on the expected loading conditions. In the case of the commuter rail system, instrumentation was installed on two different crosstie designs. However, the design philosophy for all the crossties are the same. Some key geometrical and material properties of each of the crossties studied in this project are shown in Table 1. As shown in Table 1, similar high strength concrete and prestressing steel are used in all the different crossties according to the suppliers. While a crosstie spacing of 30 in. (76.20 cm) is used in MetroLink, both NYCTA and Metra use 24 in. spacing (60.96 cm). No obvious cracking of the crossties was observed during instrumentation at all three sites.

An automated data collection system was installed at each site. This yielded exhaustive databases of information spanning long periods of time (up to 10 months). Fig. 2(a) shows a typical instrumentation plan. Additionally, Fig. 2(b) presents a photo of one of the sites after installation of the proposed instrumentation.

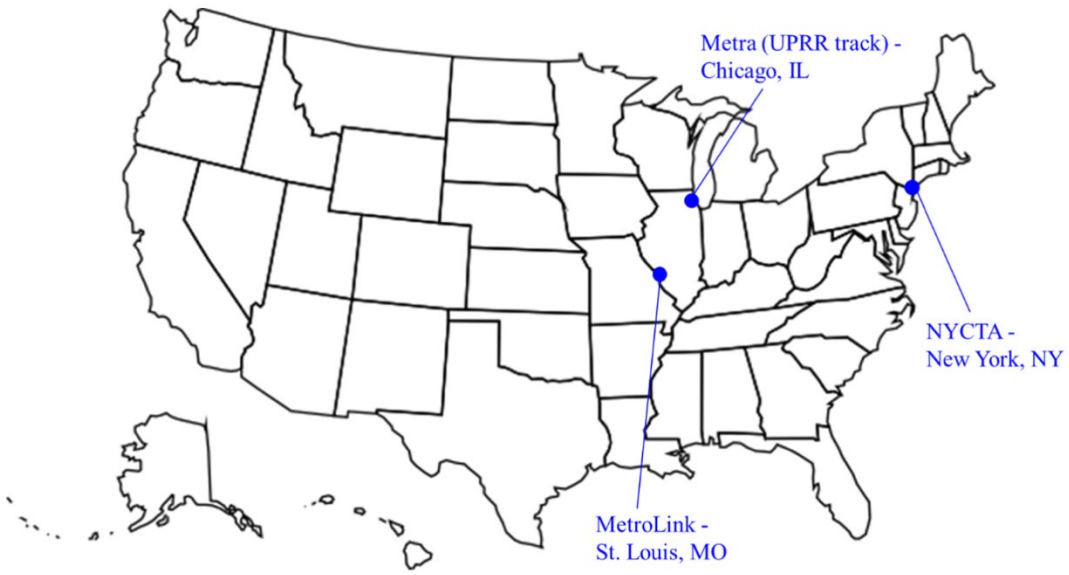

Fig. 1. Field instrumentation locations.

Table 1
Design and manufacture properties of the studied concrete crosstie designs.

Rail Transit System			MetroLink		NYCTA		Metra			
Sleeper Design			Design 1		Design 2		Design 3		Design 4	
			Imperial	SI	Imperial	SI	Imperial	SI	Imperial	SI
Cross Section Geometry	Center	Height	6.25″	0.16 m	6.75″	0.17 m	6.75″	0.17 m	8.27″	0.21 m
		Top Width	7.75″	0.20 m	7.50″	0.19 m	7.50″	0.19 m	8.23″	0.21 m
		Bottom Width	10.38″	0.26 m	10.50″	0.27 m	11.00″	0.28 m	10.50″	0.27 m
	Rail Seat	Height	8.00″	0.20 m	8.56″	0.22 m	9.00″	0.23 m	9.00″	0.23 m
		Top Width	7.38″	0.19 m	8.44″	0.21 m	7.50″	0.19 m	9.50″	0.24 m
		Bottom Width	10.38″	0.26 m	10.50″	0.27 m	11.00″	0.28 m	12.00″	0.30 m
Longitudinal Geometry	Length		8′ 3″	2.51 m	8′ 6″	2.59 m	8′ 6″	2.59 m	8′ 0″	2.44 m
	Gauge		4′ 8½″	1.44 m	4′ 8½″	1.44 m	4′ 8½″	1.44 m	4′ 8½″	1.44 m
Design Concrete Compressive Strength at 28 Days			7,000 psi	48,263 kN/m^2	7,000 psi	48,263 kN/m^2	7,000 psi	48,263 kN/m^2	8500 psi	58,605 kN/m^2
Prestressing	Number of Tendons		12		18		20		12	
	Jacking Force		7 kips	31.1 kN	7 kips	31.1 kN	7 kips	31.1 kN	11 kips	48.0 kN
	Precompression (Crosstie Center)		1.48 ksi	10,204 kN/m^2	2.01 ksi	13,858 kN/m^2	2.24 ksi	15,444 kN/m^2	1.67 ksi	11,514 kN/m2
Design Capacity	Center Negative		147 kip-in	16.6 kN-m	194 kip-in	21.9 kN-m	230 kip-in	26.0 kN-m	232 kip-in	26.2 kN-m
	Center Positive		105 kip-in	16.3 kN-m	132 kip-in	14.9 kN-m	186 kip-in	21.0 kN-m	223 kip-in	25.2 kN-m
	Rail Seat Positive		221 kip-in	25.0 kN-m	283 kip-in	32.0 kN-m	381 kip-in	43.1 kN-m	317 kip-in	35.8 kN-m
	Rail Seat Negative		136 kip-in	15.4 kN-m	178 kip-in	20.1 kN-m	219 kip-in	24.7 kN-m	244 kip-in	27.6 kN-m
Year of Manufacture			2003		2006		2003		2016	

Surface strain gauges were installed at the top chamfer of the selected concrete crossties. Through calibration with laboratory experimentation, the bending moment imposed by revenue service loads can be calculated from the measured strain as described in Eq. (1) [16]. Based on the application of the Euler-Bernoulli beam theory for small deformations, the stress distribution within the critical cross sections of the crossties is known.

$$M_s = \frac{\varepsilon_s E_c I_s}{d_s} = k\varepsilon_s \tag{1}$$

where:

- M_s is the sleeper bending moment at section "s" (kip-in (kN-m))
- ε_s is strain measurement taken from the surface strain gauge at section "s" (in/in (m/m))
- E_c is the elastic modulus of the concrete (psi (kPa))
- I_s is the moment of inertia at section "s" (in^4 (m^4))
- d_s is the distance from the surface strain gauge to the neutral axis of bending of the sleeper at section "s" (in (m))
- k is the calibration factor at section "s" (kip-in (kN-m)).

The corresponding calibration factors for each crosstie design used to convert field-obtained strains into bending moments were obtained in the laboratory following procedures described in a previous publication [16]. This methodology was used to obtain all the field bending moment data presented in this paper. The strain gauges were installed at critical sections of the crossties, the center and the rail seats. These locations are hereafter referred as "center", "rail seat A" and "rail seat E" respectively. The strain gauge configuration can be found in Fig. 3(a). The strain gauges used in this study are PFL-30-22-3LT, which are manufactured by Tokyo Sokki Kenkyujo Co, Ltd. These gauges are designed for concrete surface applications. Calibration factors used in this investigation are shown in Table 2.

Thermocouples were installed on the top chamfer and the base of crosstie 6 as marked in Fig. 2(a). The thermocouples arrangement on the crosstie is sketched in Fig. 3(b). The thermocouples were installed to measure the temperature variation at the top and bottom of the center of the crosstie only due to the limited availability of channels feeding into the data acquisition system. However, all the measured crossties presented direct exposure to exterior conditions, and, as shown in Table 1, crossties are not particularly long. Therefore, constant temperature along the whole length of the crossties at top and bottom was assumed for the presented analysis. Additionally, the ambient temperature was recorded to address its relationship with the temperature of the crossties. The temperature was recorded in 5–15 min intervals. National Instruments (NI) 9135 Automated Compact Data Acquisition (cDAQ) system was used to collect data automatically with a laser trigger supplied by Micro-Epsilon whenever a train passed by the site.

3. Results and discussion

3.1. Temperature variation in concrete crossties placed in track

Table 3 shows the start and end date of temperature data collection at each site, as well as the total number of days with stored data. Note that temporary interruptions occurred occasionally during data collection.

Fig. 4 depicts the ambient, crosstie top, and crosstie bottom temperature data collected from each site. Highest temperatures are found at the top of the crosstie where it is exposed to solar radiation. Fig. 4(a) shows an overview of the collected tempera-

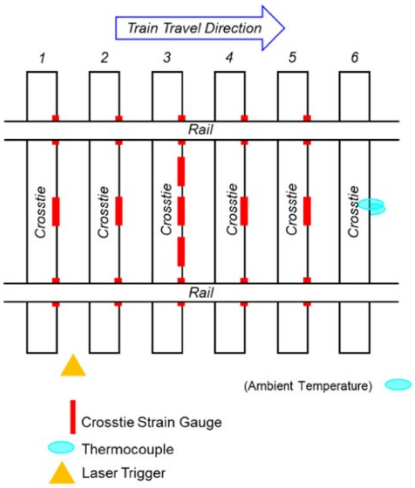

(a). Schematic drawing of a field instrumentation plan.

(b). Photo of an instrumented site.

Fig. 2. Example of the field instrumentation.

ture data at the light rail system at MetroLink. The temperature at the top of the crosstie largely exceeds the temperature at the bottom of the crosstie and the ambient temperature. This is a consistent trend that can be observed for both hot (e.g. June and July) and cold periods (e.g. January). Fig. 4(b) presents the temperature variation over time recorded at the heavy rail track (NYCTA). Spanning over 10 months, the temperature database presents similar trends to the data that was found at MetroLink. It is shown that the ambient temperature drives the temperature variation along the crosstie, both top and bottom. Additionally, the largest temperatures are found at the top of the crosstie, where wide temperature variation takes place. The temperature variation over time at Metra is presented in Fig. 4(c). Despite the shorter monitoring period with respect to the previous cases, this site gives the possibility of comparing two different types of crossties subjected to the same environmental and loading conditions. The temperature distribution at the top and bottom of the crossties shows very similar patterns for the two different designs of crossties. In this case, it should be noted that the temperature at the top of the crossties is quite similar to the temperature at the bottom, which usually falls below the ambient temperature.

The three sites present similar types of track and field instrumentation setups. However, when comparing the three different site results, the most remarkable difference is the correlation between the top and ambient temperature. For MetroLink and NYCTA, the data shows that typically the crosstie top temperature is higher than the ambient temperature. This is not the case for Metra. The difference can be explained by the presence of ballast particles laying on top of the crossties. Due to the different track maintenance practices, it shows an effect on the temperature of the crosstie when the crosstie is covered by ballast particles or

Table 2
Laboratory obtained calibration factors.

Rail Transit System		Calibration Factor (k)	
Sleeper Design		Imperial	SI
MetroLink "Design 1"	Center	−398,851.31 kip-in	−45,064.15 kN-m
	Rail Seat	−731,491.44 kip-in	−82,647.44 kN-m
NYCTA "Design 2"	Center	−529,103.32 kip-in	−59,780.65 kN-m
	Rail Seat	−917,161.93 kip-in	−103,625.38 kN-m
Metra "Design 3"	Center	−504,946.71 kip-in	−57,051.32 kN-m
	Rail Seat	–	–

Table 3
Summary of data collection at the different studied rail transit locations.

Site	First Day	Last Day	Total Number of Days
MetroLink	03/07/2016	10/19/2016	175
NYCTA	04/26/2016	02/27/2017	224
Metra	08/04/2016	04/03/2017	96

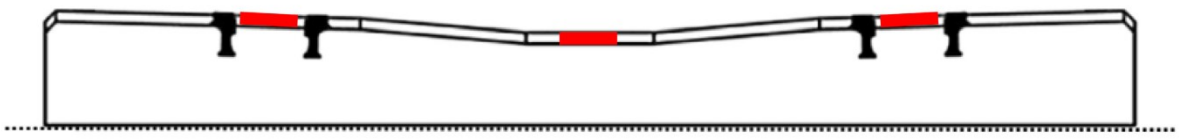

(a). Typical configuration of strain gauges installed on concrete crossties.

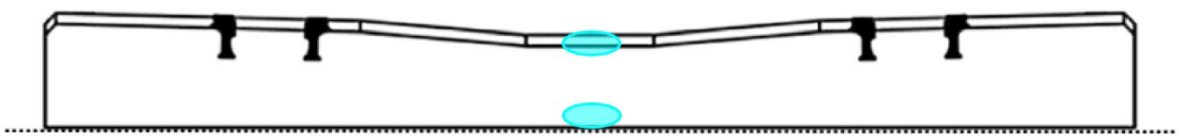

(b). Configuration of thermocouples on concrete crossties.

Fig. 3. Configurations of strain gauges and thermocouple installed in crossties.

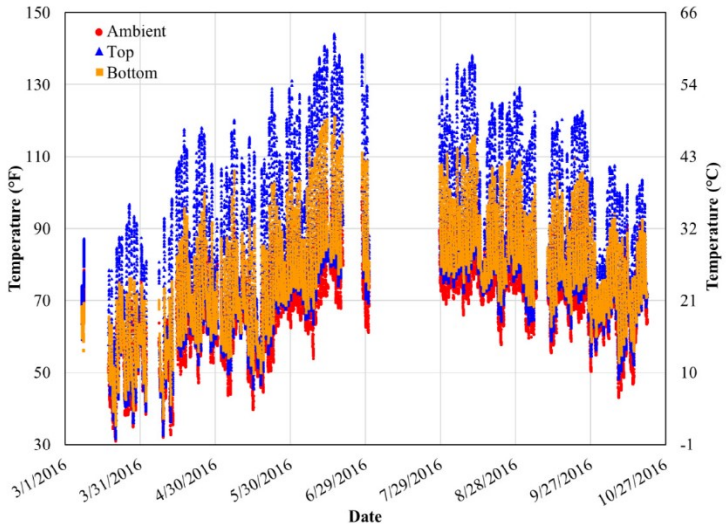

(a) Temperature distribution in crossties at MetroLink.

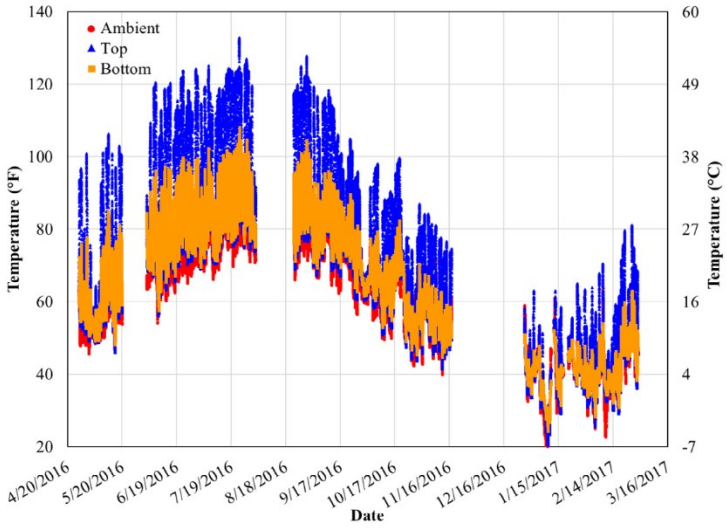

(b) Temperature distribution in concrete crossties at NYCTA.

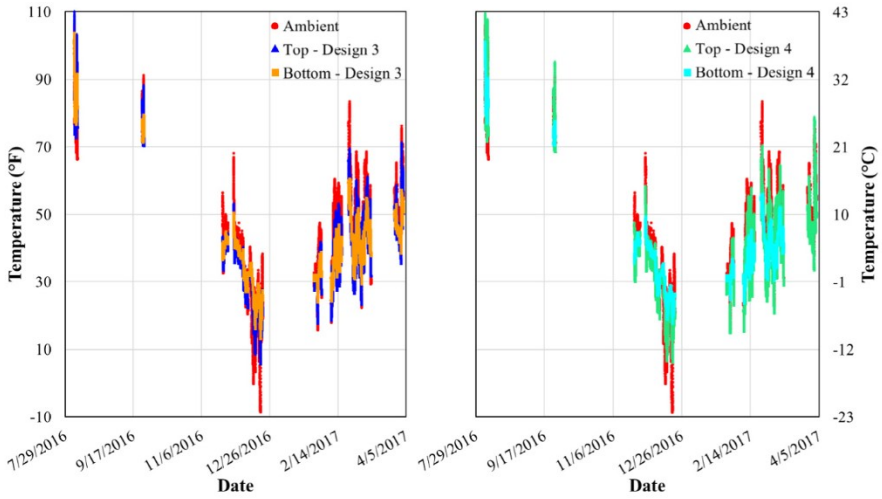

(c) Temperature distribution in crossties at Metra.

Fig. 4. Temperature distribution observed in crossties from each field experimentation site.

not. When the crosstie is directly exposed to the solar radiation, higher temperatures on top of the crosstie can be reached, up to 144.1 °F (62.3 °C) in this study. On the other hand, when the ballast particles are laid on top of the crosstie, the aggregates absorb a considerable portion of the radiation, having a lower temperature in the middle portion of the crosstie with respect to the ambient

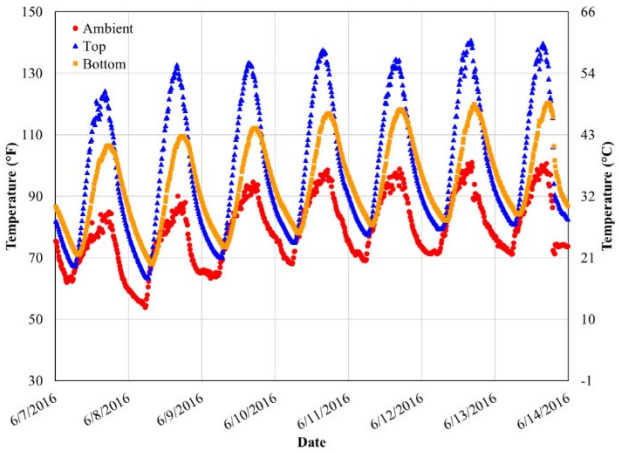

(a) Temperature fluctuation during the warmest week in MetroLink.

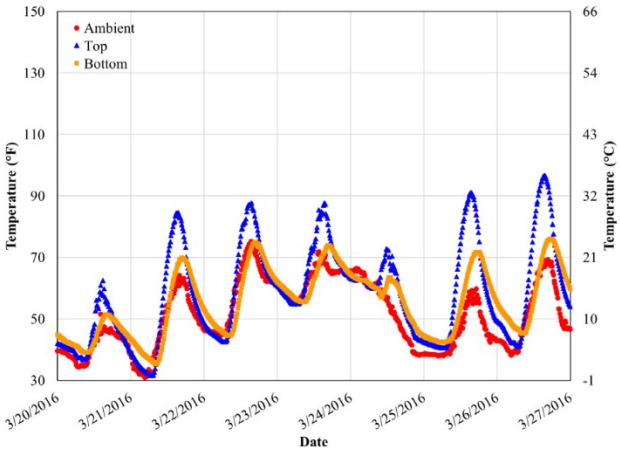

(b) Temperature fluctuation during the coolest week in MetroLink.

Fig. 5. Ambient, crosstie top, and bottom temperature variation in MetroLink during the warmest and coolest weeks of the recorded dataset.

temperature. The direct radiation to the crosstie not only causes temperature on top of the crosstie to increase, but also propagates to the bottom of the crosstie. In consequence, higher temperatures along the middle section of the crosstie are observed.

Other than the temperature variation throughout the entire data collection period, it is also necessary to understand daily temperature fluctuations. A week of temperature data from Metrolink that corresponds to the warmest and coolest week respectively is presented in Fig. 5. The crosstie top and bottom temperature variation with respect to the ambient temperature for the two extreme cases can be compared.

Fig. 5 indicates that for higher ambient temperatures, the temperature gradient within the crosstie (i.e. the temperature difference between the top and bottom) is larger. Note that the bottom temperature tends to be higher than the ambient temperature during warmer periods too. Daily temperature fluctuations are observed and a clear pattern can be identified for the temperature measured at the three different locations.

When focusing on one day instead of one week, it can be observed in Fig. 5 that the top temperatures increase at a higher rate than the bottom temperatures toward the middle of the day. Hence, the maximum temperature gradient is found around noon to the early afternoon due to a large increase of the temperature at the top of the crosstie. Given that this period is coincident with the period of intense solar radiation, a qualitative relation can be inferred. A consistent trend is discovered as, during the daytime, the crossties undergo positive temperature gradients. These trends are specifically related to the solar radiation heating up the top of the crosstie. Moreover, the night periods present the smallest positive gradients and a large number of negative gradients. Table 4 summarizes the maximum, minimum, and average of the recorded ambient temperatures, crosstie top and bottom temperature, and the corresponding temperature gradient for the four different crossties in this study.

As shown in Table 4, the ambient temperature shows similar values for the three sites with the exception of significantly colder temperatures found in Metra in late December 2016. Nonetheless, the maximum values of the temperature are larger at top and bottom of the crosstie for MetroLink and NYCTA. This difference, that has been explained earlier, is a result of the placement of ballast on top of the crossties at the track crib or not. In a similar way, maximum positive gradients (i.e. top temperature minus bottom temperature) are found to be higher for MetroLink and NYCTA.

In Fig. 6, the top and bottom temperatures are plotted versus the ambient temperature for the four types of crossties. The top temperature regression slope is higher as it varies more rapidly (or at a higher rate) than the one at the bottom. In other words, the temperature at the top of the crosstie is more sensitive to the ambient temperature as compared to the temperature at the bottom of the crosstie. An apparent linearity of all the datasets can be observed when comparing temperature at the crosstie versus ambient temperature. Hence, to describe the relationship between top and bottom temperature at the different crossties along with corresponding ambient temperatures, linear regression was performed. The obtained equations and the coefficient of determina-

Table 4
Summary of field measured temperatures on concrete crossties for the four different sites.

Site		Ambient		Top		Bottom		Gradient	
		°F	°C	°F	°C	°F	°C	°F	°C
MetroLink (Design 1)	Maximum	105.1	40.6	144.1	62.3	121.0	49.4	32.2	17.9
	Minimum	31.0	−0.6	31.7	−0.2	35.3	1.8	−12.1	−6.7
	Average	67.3	19.6	70.8	21.6	68.0	20.0	2.8	1.6
New York NYCTA (Design 2)	Maximum	98.3	36.8	132.7	55.9	108.1	42.3	38.1	21.2
	Minim5um	18.2	−7.7	20.4	−6.4	24.3	−4.3	−9.7	−5.4
	Average	60.6	15.9	67.0	19.4	64.7	18.2	2.3	1.3
Metra (Design 3)	Maximum	106.2	41.2	115.2	46.2	103.6	39.8	18.4	10.2
	Minimum	−8.5	−22.5	5.6	−14.7	13.1	−10.5	−14.9	−8.3
	Average	41.8	5.4	39.7	4.3	40.6	4.8	−2.1	−1.2
Metra (Design 4)	Maximum	106.2	41.2	121.1	49.5	101.1	38.4	24.1	13.4
	Minimum	−8.5	−22.5	6.2	−14.3	17.6	−8.0	−13.8	−7.7
	Average	41.8	5.4	39.1	3.9	39.4	4.1	−1.4	−0.8

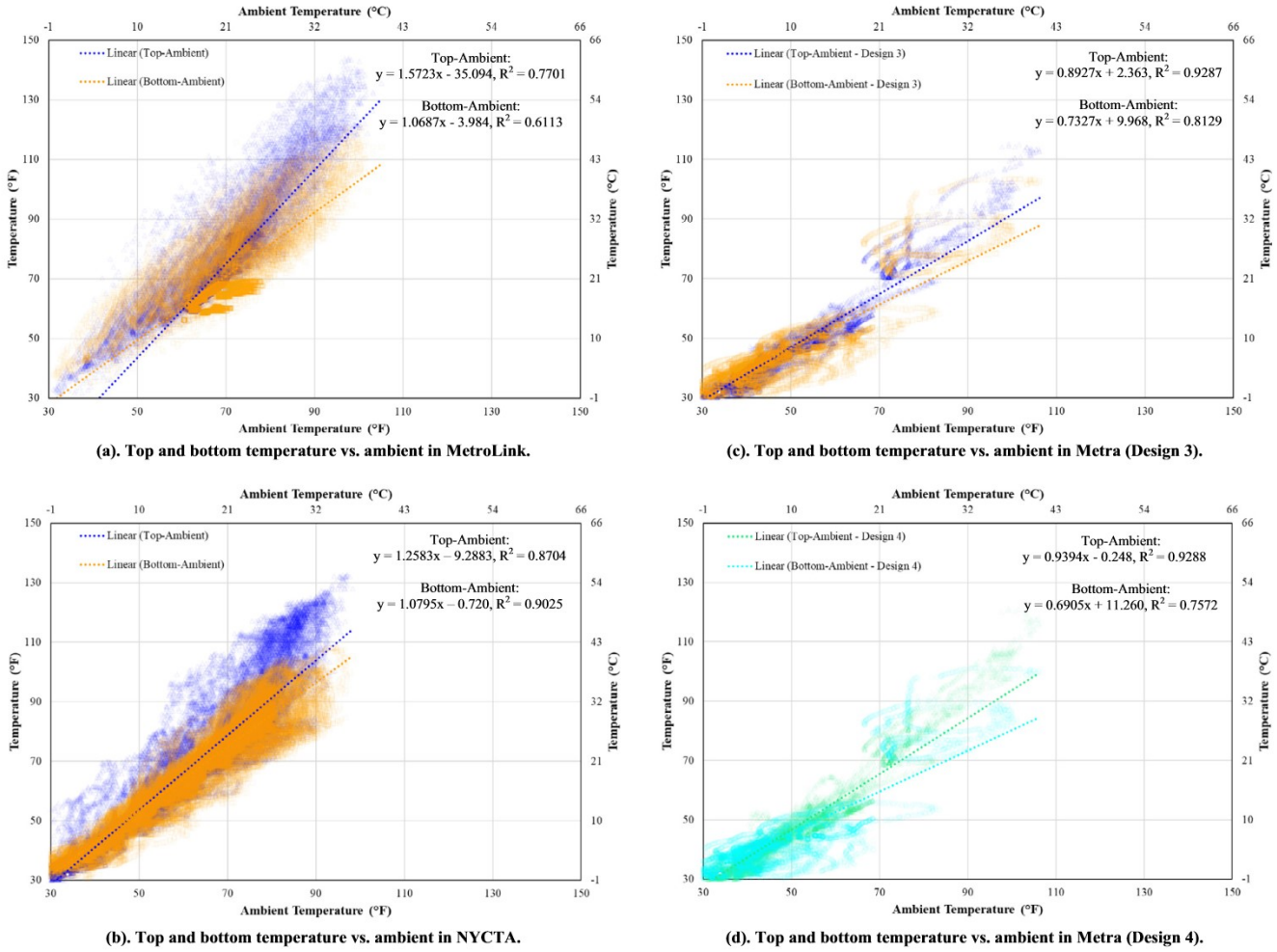

Fig. 6. Linear relation of top and bottom temperature with ambient temperature for the four crosstie designs in the scope of study.

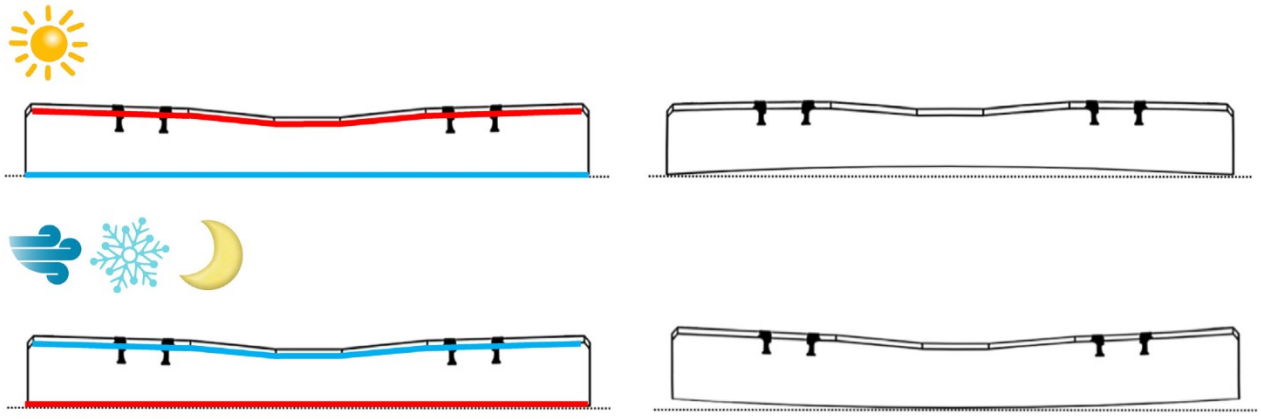

Fig. 7. Graphical representation of crosstie deformation subjected to temperature gradients.

tion (R^2) are shown in Fig. 6. The equations and coefficient of determination represent the dispersion of data with respect to the linear regression.

Values of R^2 were found to range from 0.61 to 0.93. Given the large dataset, the extensive monitoring period, and the repetition in this study for different cases, it is safe to say that the relationship between top temperature and ambient temperature, as well as bottom temperature and ambient temperature, can be deemed as linear. In addition, it can be observed that the presence of ballast on the top of the crib makes a difference in the overall temperature distribution of the crosstie. The direct solar radiation on the crosstie yields consistently higher top temperatures than the ambient temperature. This is expressed through a larger slope of the linear trend line. Because the top of the crosstie is warmer, and the bottom is colder, heat can propagate from the top to the bottom of the crosstie. This results in slopes greater than one for MetroLink and NYCTA. The results for the two crosstie designs at Metra present very similar results. For both cases, the top temperature tends to

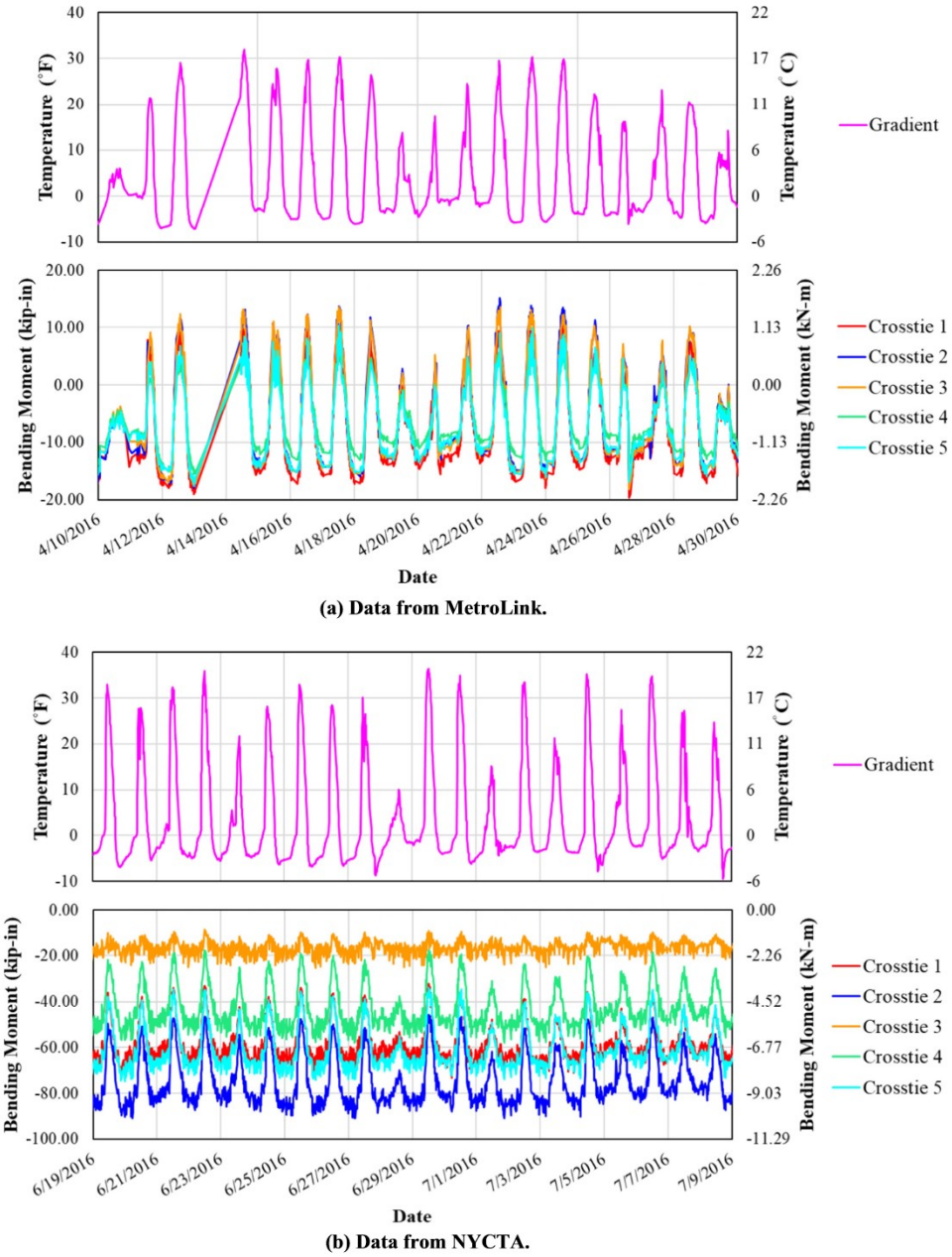

Fig. 8. Temperature gradient and center bending moment variation over time.

fall below the value of the ambient temperature as the solar radiation does not directly hit the middle portion of the crosstie. The relationship between ambient temperatures and temperatures within crossties could assist the concrete crosstie industry in future designs for specific regions considering the temperature in a similar approach to what has been used for concrete girder, pavement, and frame designs.

3.2. Temperature effect on crosstie support conditions and flexural behavior

The flexural behavior of crossties heavily depends on the support conditions. Previous research on concrete crosstie flexural behavior has proven the importance of ballast support conditions. Ballast support conditions largely affect the resultant bending moment [17,18]. The effect of the temperature gradient on the support conditions has been proven in an earlier study [12], which is explained in Fig. 7. In Fig. 7, the higher temperatures are marked in red and the lower temperatures are marked in blue. When the top of the crosstie gets warmer than the bottom due to solar radiation, a higher elongation occurs on the top causing the crosstie to lose contact with the support at the center. The opposite case happens during nighttime, or under cold temperatures induced by weather conditions (e.g. wind, snow), that causes the top to be colder than the bottom. This leads to an opposite effect, shifting the support conditions towards center binding scenario, as the crosstie starts to lose contact from the two ends. However, while the temperature gradient between top and bottom plays a key role on the variation of the support conditions, the uniform deformation of the crosstie (i.e. expansion or retraction) also affects the contact between the ballast and the crosstie.

Fig. 8 presents the variation of the concrete crosstie center bending moments under revenue service along with the corresponding temperature gradient for MetroLink and NYCTA over a

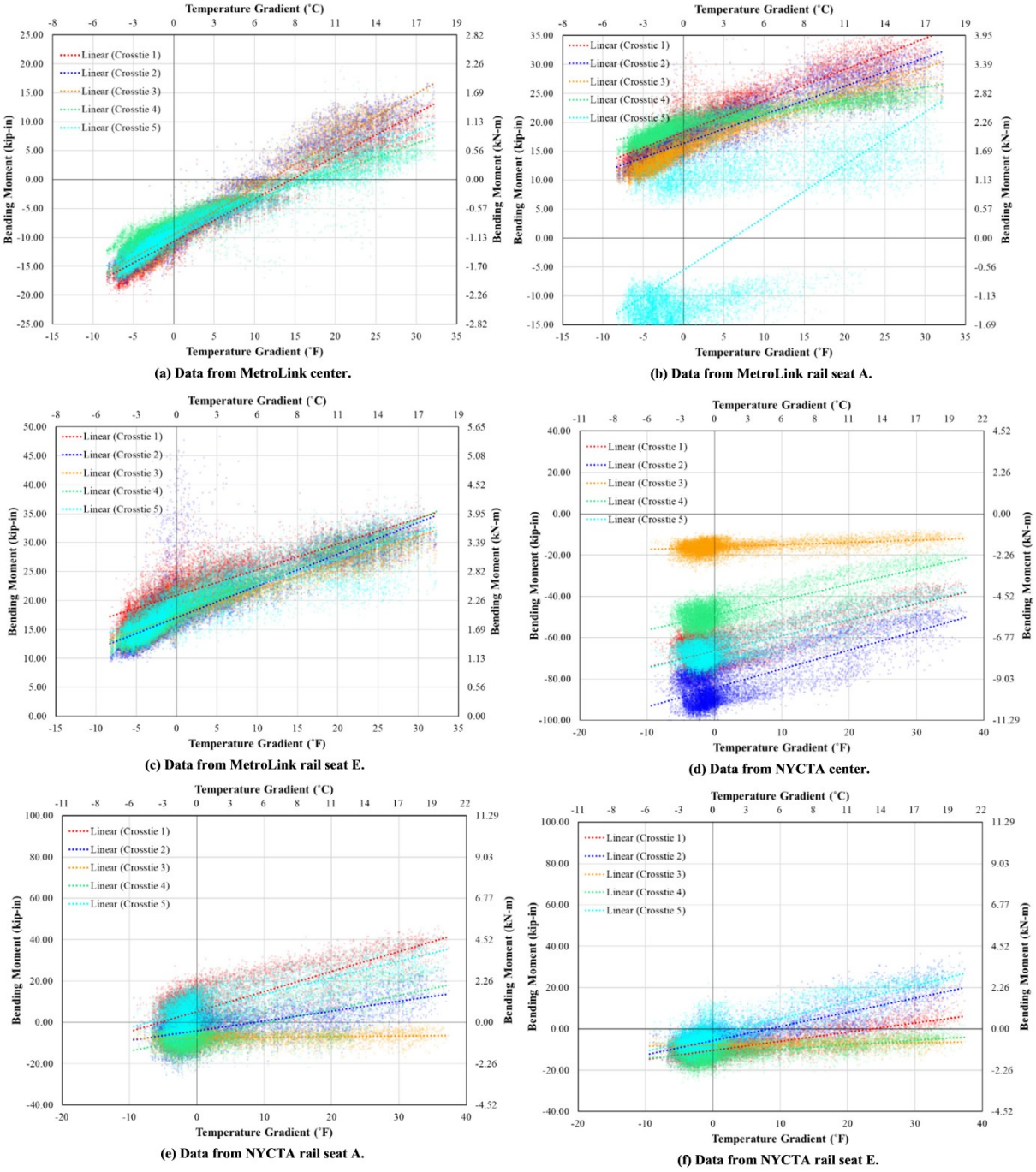

Fig. 9. Bending moment versus temperature gradient.

period of 20 days. As mentioned earlier, insufficient bending moment data was collected from Metra to plot a similar graph due to track access issues and other field challenges. While MetroLink presents similar bending moment results among crossties, the same trend was not found at NYCTA. It is interesting to note that the variation of concrete crosstie center bending moments and the variation of the corresponding temperature gradient follow exactly the same pattern, suggesting a strong relationship between both variables.

In order to quantify the possible relationship indicated by Fig. 8, concrete crosstie bending moment versus temperature gradient for all the data collected from MetroLink, NYCTA, and Metra "Design 3" crossties is presented in Fig. 9. Strong linear correlations are seen as shown in Fig. 9 and details are summarized in Table 5, including the regression equations as well as the corresponding R^2 values.

Not only there is a strong linear correlation between bending moment and temperature gradient shown in Fig. 9, it is also remarkable that the center bending moment at the light rail system shifts from negative to positive values. An absolute variation of 30 kip-in (3.39 kN-m), from −17 kip-in (−1.92 kN-m) to 13 kip-in (1.47 kN-m), is found for a shift in the temperature gradient from −7 °F (−3.9 °C) to 30 °F (16.7 °C). When compared with the design capacity for the center negative bending moment of the "Design 1", used for MetroLink, this bending moment variation due to temperature effects represents 21% of the design capacity.

For the heavy rail system, similar slopes are found for 4 out of the 5 crossties at the center, where crosstie 4 shows the highest percentage of the overall bending moment variation. An increase of 38 kip-in (4.29 kN-m) is found for a shift in the temperature gradient from −10 °F (−5.6 °C) to 37 °F (20.6 °C). As noted before, NYCTA uses "Design 2", whose center negative bending moment capacity is 194 kip-in (21.69 kN-m). Hence, an increase in the flexural demand in the center as found in the field would represent up to 20% of the design capacity of the crosstie. Results from the Metra site using "Design 3" under both commuter rail and freight revenue service loading also presents similar linear trends as the other transit modes. A higher level of dispersion is present in these data. This could be due to a smaller dataset, higher variation in the loading environment (mixed commuter trains and freight train operation), or lower quality of the data. Nevertheless, a maximum center bending moment variation of 13 kip-in (1.47 kN-m) over a temperature gradient variation of 22 °F (12.2 °C) is observed, which represents up to 11% of the design capacity.

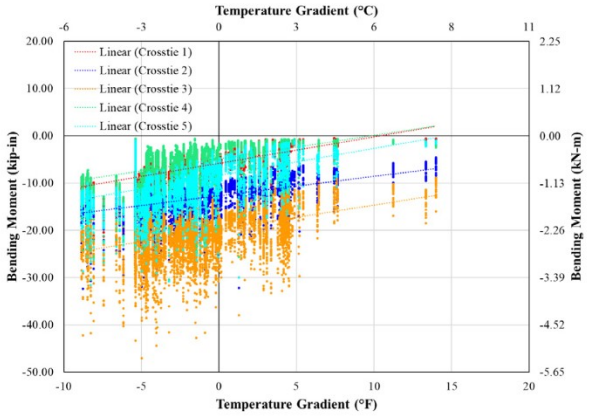

(g) Data from Metra (Design 3) center.

Fig. 9 (*continued*)

With the exception of crosstie 3 in the NYCTA's field setup, the data shows strong linearity according to the R^2 values. This linearity is more blatant for the center bending moment, as fewer factors affect the results at this section with respect to the rail seat. First, the deformation of the crosstie under revenue service loading can change support conditions, showing larger variability in the rail seat results. In addition to this, the rail seat load distribution, usually idealized as point load or distributed load, varies [19], affecting the bending moment at the cross section. It is known that deep beam behavior is found at the rail seat cross section, and the angle of dispersion of the compressive field has been proven to be function of the load and the support conditions [20]. Besides, from the instrumentation point of view, it is extremely difficult to install strain gauges under the rail seat in the field under traffic, likely resulting in less precise positioning and alignment compared to installation of center gauges. In addition, variability in the field testing, homogeneous temperature variation in the crosstie, or the change in the dynamic input load are factors that cause dispersion in the data.

As a linear relation between bending moment and the temperature gradient is shown based on field results, additional research was conducted to develop a numerical simulation to provide further insight into these trends. A finite element (FE) model developed under previous research [12,21,22] was used to analyze the relation between temperature gradient and crosstie curling [12]. This FE model developed in ABAQUS, defines the crosstie-ballast interaction using contact pairs. The used coefficient of friction (COF) was 0.7, based on experimental data. Details of the previously developed FE model can be found in the aforementioned literature. Several cases were run for gradients ranging from −10 °F (−5.56 °C) to 30 °F (16.67 °C) to quantify the bending moment at the crosstie center with the assumption that the crosstie is evenly supported along its length. Fig. 10 shows the results of the FE analysis.

It can be observed in Fig. 10 that a linear relation between bending moment and temperature gradient is confirmed when keeping the loading the same. Note that the loading environment was determined to be consistent for all sites in this study through

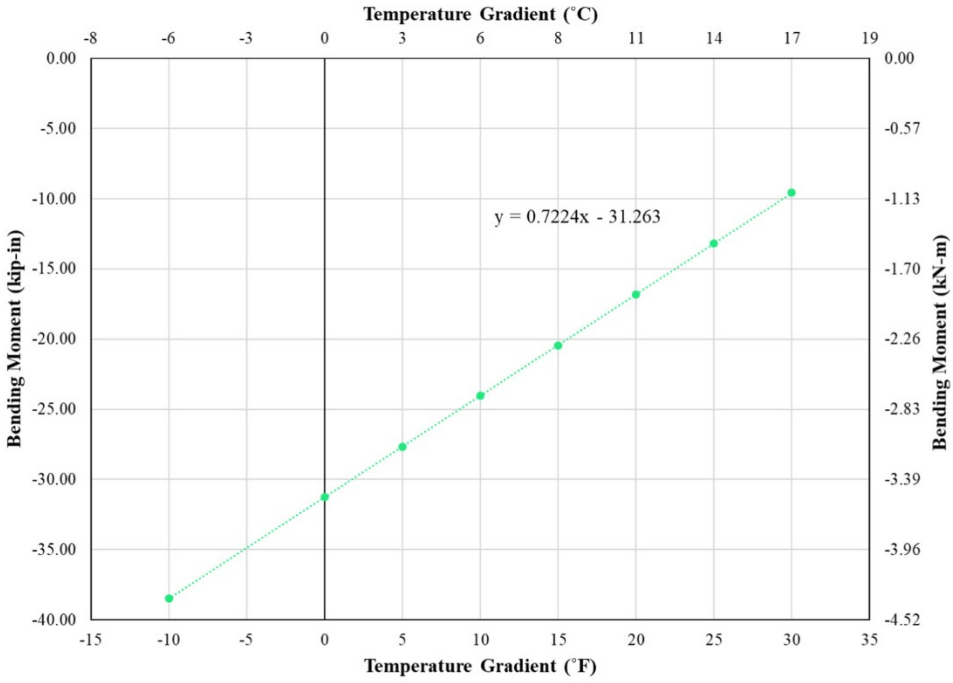

Fig. 10. Temperature gradient versus center bending moment obtained through numerical simulation.

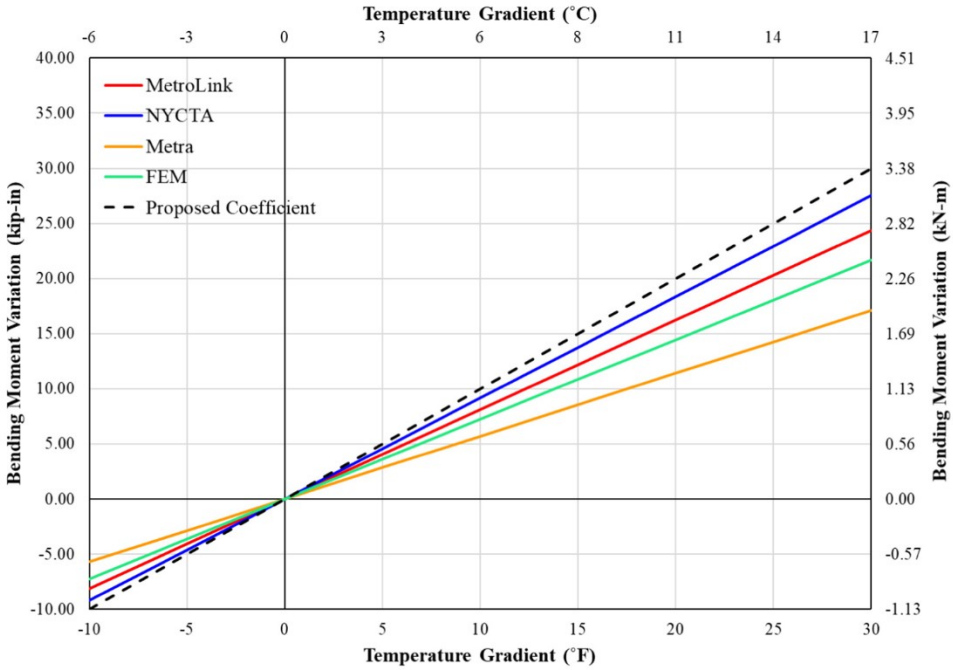

Fig. 11. Comparison of field results, numerical simulation results, and proposed correction factor for design.

Table 5
Linear regression results for bending moment versus temperature gradient.

Site			Center	Rail Seat A	Rail Seat E
St. Louis MetroLink	Crosstie 1	Eq.	y = 0.7373x – 10.73	y = 0.5407x + 18.341	y = 0.4442x + 20.907
		R^2	0.9470	0.8488	0.7550
	Crosstie 2	Eq.	y = 0.8111x – 9.5037	y = 0.494x + 16.377	y = 0.5474x + 17.037
		R^2	0.9529	0.8272	0.7189
	Crosstie 3	Eq.	y = 0.8117x – 9.482	y = 0.4697x + 15.429	y = 0.5569x + 17.424
		R^2	0.9540	0.8720	0.9190
	Crosstie 4	Eq.	y = 0.4822x – 8.2182	y = 0.2368x + 18.98	y = 0.4654x + 17.197
		R^2	0.8558	0.7609	0.8514
	Crosstie 5	Eq.	y = 0.6089x – 9.8827	y = 0.9113x – 5.5686	y = 0.4506x + 18.234
		R^2	0.9208	0.4379	0.6914
MTA New York City Transit	Crosstie 1	Eq.	y = 0.7662x – 66.720	y = 0.9692x + 5.173	y = 0.4411x – 10.539
		R^2	0.5282	0.5842	0.6158
	Crosstie 2	Eq.	y = 0.9176x – 84.405	y = 0.4731x – 4.091	y = 0.6878x – 5.741
		R^2	0.5735	0.3884	0.6838
	Crosstie 3	Eq.	y = 0.1135x – 16.224	y = 0.0286x – 7.569	y = 0.0418x – 8.004
		R^2	0.1414	0.0092	0.0290
	Crosstie 4	Eq.	y = 0.7413x – 49.000	y = 0.6735x – 7.197	y = 0.2141x – 12.090
		R^2	0.6186	0.5394	0.2742
	Crosstie 5	Eq.	y = 0.7851x – 66.859	y = 0.7999x + 5.570	y = 0.797x – 2.978
		R^2	0.6852	0.5852	0.7077
Chicago Metra (Design 3)	Crosstie 1	Eq.	y = 0.5598x – 5.8173	N/A	N/A
		R^2	0.3599		
	Crosstie 2	Eq.	y = 0.4138x – 12.684	N/A	N/A
		R^2	0.2030		
	Crosstie 3	Eq.	y = 0.5153x – 19.791	N/A	N/A
		R^2	0.1774		
	Crosstie 4	Eq.	y = 0.4991x – 4.9044	N/A	N/A
		R^2	0.2198		
	Crosstie 5	Eq.	y = 0.5704x – 8.37	N/A	N/A
		R^2	0.2182		

long-term monitoring [23]. The slope of the linear regression, shown in Fig. 10, also falls within the range of values derived from the field data presented in Table 5. Thus, it is reasonable to conclude that the effect of the temperature on the flexural behavior of concrete crossties under revenue service loading conditions has a linear correlation. This correlation is primarily dependent on the temperature difference between top and bottom of the crosstie.

As discussed earlier, based on the data collected from the field in this study, the variation of crosstie bending moment could be

up to 20% of the design capacity due to the temperature gradient. It is expected that with a higher temperature gradient, the variation of bending moment would account for a higher percentage of the designed capacity. Therefore, it is not safe to ignore the effect of temperature gradients in the design process of concrete crossties considering they are usually placed in demanding territories. Based on the field data collected in this study, the results presented in Table 5, and the numerical simulations results shown in Fig. 10, a *Correction Factor* of 1 kip-in/°F (0.203 kN-m/°C) is proposed. Hence, for bending moment capacity design, an increment equal to the temperature gradient between the top and bottom times the proposed coefficient should be added to account for bending moment variation due to the temperature induced support conditions changes. A comparison of the maximum effect on the center bending moment found in the field and the proposed *Correction Factor* is shown in Fig. 11. The proposed correction factor represents a slightly conservative approach. For design purposes, the proposed correction factor should be coupled with a predicted temperature gradient considering the most extreme environmental conditions in specific regions.

4. Conclusions

An extensive field study of temperature effects on concrete crossties for rail transit applications has been conducted. Using instrumentation installed on three different transit properties for collection of revenue service train data, the investigation comprised different loading scenarios as well as support conditions. The following conclusions can be drawn:

The temperature at the top and bottom of the four types of crossties showed a close linear relation with the ambient temperature. Additionally, the temperature at the top chamfer of the crosstie is generally higher than the temperature at the base. The presence of ballast on the top of the crib prevents the top of the crosstie from direct solar radiation yielding lower temperatures at the top chamfer and base for similar ambient temperatures.

The largest positive gradients are found towards the middle of the day (12:00 noon) and are associated with solar radiation. Negative gradients are often found during the nighttime hours. With the selected instrumentation sites, the maximum positive temperature gradient (top chamfer temperature minus base temperature) found in the field was 38.1 °F (21.2 °C). The largest negative temperature gradient found in the field was −12.1 °F (−6.7 °C). When comparing absolute values, positive temperature gradients are larger than the negative temperature gradients.

The relation between temperature variation and flexural behavior of concrete crossties under revenue service loading conditions has been shown to be linear and consistent among different sites. The bending moment variation at the center and the rail seats for a given temperature gradient variation is found to be similar for different loading environments and concrete crosstie designs. Positive temperature gradients cause a reduction of the center negative bending moment, and an increase of the rail seat positive bending moment. This has been attributed to a loss of contact around the center region (and increase towards the rail seats) of the crosstie with the ballast due to the positive bowing of the element.

Variation of bending moment at the center of the crosstie due to temperature gradient ranges from 11% to 21% of the crosstie design capacity based on the field data collected in this study. Design methodologies should acknowledge the importance of temperature-related effects on crossties flexural behavior. A *Correction Factor* of 1 kip-in/°F (0.203 kN-m/°C) is proposed to account for the change in support conditions due to the temperature gradient. The proposed *Correction Factor* needs to be coupled with a predicted temperature gradient considering the most extreme environmental conditions in specific regions.

Conflict of interest

None.

Acknowledgments

Portions of this research effort were funded by the Federal Railroad Administration (FRA) and the Federal Transit Administration (FTA), both part of the United States Department of Transportation (US DOT). The material in this paper represents the position of the authors and not necessarily that of FRA or FTA. Track access was granted by MetroLink, NYCTA, and Union Pacific Railroad. The authors would like to express their gratitude for the financial and field instrumentation support. The authors would also like to thank Matt Csenge, Xiao Lin, Aaron Cook, and other research assistants in RailTEC at UIUC for their assistance in field instrumentation. J. Riley Edwards has been supported in part by grants to UIUC's RailTEC from CN and Hanson Professional Services, Inc.

References

[1] W.W. Hay, Railroad Engineering, 2nd ed., Wiley, New York, NY, USA, 1982.
[2] Z. Gao, H.E. Wolf, M.S. Dersch, Y. Qian, J.R. Edwards, Field measurements and proposed analysis of concrete crosstie bending moments Orlando, FL, USA, Proceedings of the American Railway Engineering and Maintenance-of-Way Association Annual Conference, 2016.
[3] P.J. Barr, J.F. Stanton, M.O. Eberhard, Effects of temperature variations on precast, prestressed concrete bridge girders, J. Bridge Eng. 10 (2005) 186–194, https://doi.org/10.1061/(ASCE)1084-0702(2005)10:2(186).
[4] F.J. Vecchio, J.A. Sato, Thermal gradient effects in reinforced concrete frame structures, ACI Struct. J. 87 (1990) 262–275.
[5] E.H. El-Tayeb, S.E. El-Metwally, H.S. Askar, A.M. Yousef, Thermal analysis of reinforced concrete beams and frames, HBRC J. 13 (2017) 8–24, https://doi.org/10.1016/j.hbrcj.2015.02.001.
[6] M.R. Thompson, B.J. Dempsey, H. Hill, J. Vogel, Characterizing temperature effects for pavement analysis and design, Trans. Res. Rec.: J. Trans. Res. Board (1987) 14–22.
[7] J.M. Armaghani, T.J. Larsen, L.L. Smith, Temperature response of concrete pavements, Trans. Res. Rec.: J. Trans. Res. Board (1987) 23–33.
[8] J.M. Richardson, J.M. Armaghani, Stress caused by temperature gradient in portland cement concrete pavements, Trans. Res. Rec.: J. Trans. Res. Board (1987) 7–13.
[9] A.R. Mohamed, W. Hansen, Prediction of stresses in concrete pavements subjected to non-linear gradients, Cem. Concr. Compos. 18 (1996) 381–387, https://doi.org/10.1016/S0958-9465(96)00028-5.
[10] T. Yu, L. Khazanovich, M. Darter, A. Ardani, Analysis of concrete pavement responses to temperature and wheel loads measured from intrumented slabs, Trans. Res. Rec.: J. Trans. Res. Board 1639 (1998) 94–101, https://doi.org/10.3141/1639-10.
[11] S. Rao, J.R. Roesler, Characterizing effective built-in curling from concrete pavement field measurements, J. Trans. Eng. 131 (2005) 320–327, https://doi.org/10.1061/(ASCE)0733-947X(2005) 131:4(320).
[12] H.E. Wolf, Y. Qian, J.R. Edwards, M.S. Dersch, D.A. Lange, Temperature-induced curl behavior of prestressed concrete and its effect on railroad crossties, Constr. Build. Mater. 115 (2016) 319–326, https://doi.org/10.1016/j.conbuildmat.2016.04.039.
[13] B.H. Nam, J.H. Yeon, Z. Behring, Effect of daily temperature variations on the continuous deflection profiles of airfield jointed concrete pavements, Constr. Build. Mater. 73 (2014) 261–270, https://doi.org/10.1016/j.conbuildmat.2014.09.073.
[14] M.V. Csenge, X. Lin, H. Wolf, M.S. Dersch, J.R. Edwards, Mechanistic design of concrete monoblock crossties for rail transit loading conditions, American Public Transportation Association 2015 Rail Conference, 2015. Salt Lake City, UT, USA.
[15] American Association of State Highway and Transportation Officials. AASHTO LRFD Bridge Design Specifications. 7th ed. Washington DC, USA, 2016.
[16] J.R. Edwards, Z. Gao, H.E. Wolf, M.S. Dersch, Y. Qian, Quantification of concrete railway sleeper bending moments using surface strain gauges, Meas.: J. Int. Meas. Confederation 111 (2017) 197–207, https://doi.org/10.1016/j.measurement.2017.07.029.
[17] J.R. Edwards, A.E. Canga Ruiz, A.A. Cook, Y. Qian, M.S. Dersch, Quantifying bending moments in rail-transit concrete sleepers, J. Trans. Eng., Part A: Syst. 144 (2018) 04018003, https://doi.org/10.1061/JTEPBS.0000125.
[18] Z. Gao, M.S. Dersch, Y. Qian, J.R. Edwards, Effect of track conditions on the flexural performance of concrete sleepers on heavy-haul freight railroads, 11th International Heavy Haul Association Conference, 2017. Cape Town, South Africa.
[19] A. Ghosh, M.J. Greve, M.S. Dersch, J.R. Edwards, C.P.L. Barkan, Analyzing rail seat load distributions on concrete sleepers using matrix based tactile surface

sensors Milan, Italy, Proceedings of the 11th World Congress on Railway Research, 2016.
[20] Z. Gao, Y. Qian, M.S. Dersch, J.R. Edwards, Compressive stress distribution in prestressed concrete and its effect on railroad crosstie design, Constr. Build. Mater. 151 (2017) 147–157, https://doi.org/10.1016/j.conbuildmat.2017.05.186.
[21] Z. Chen, M. Shin, B. Andrawes, J.R. Edwards, Parametric study on damage and load demand of prestressed concrete crosstie and fastening systems, Eng. Failure Anal. 46 (2014) 49–61, https://doi.org/10.1016/j.engfailanal.2014.08.002.
[22] Z. Chen, Mechanistic analysis of concrete crosstie and fastening system using field-validated finite element model. (Doctoral Thesis). University of Illinois at Urbana-Champaign, Department of Civil and Environmental Engineering, 2015.
[23] J.R. Edwards, A.A. Cook, M.S. Dersch, Y. Qian, Quantification of rail transit wheel load and development of improved dynamic and impact loading factors for design, J. Rail Rapid Transit (2018), https://doi.org/10.1177/0954409718770924.